THE JOURNAL OF PHYSICAL CHEMISTRY B LETTERS

2006, *110,* 11611−11614
Published on Web 05/28/2006

Chiroptical Activity of BINAP-Stabilized Undecagold Clusters

Yasushi Yanagimoto,[†] Yuichi Negishi,[†] Hisashi Fujihara,[‡] and Tatsuya Tsukuda*[,†,§]

Research Center for Molecular-Scale Nanoscience, Institute for Molecular Science, Myodaiji, Okazaki 444-8585, Japan, Department of Applied Chemistry and Molecular Engineering Institute, Kinki University, Kowakae, Higashi-Osaka 577-8502, Japan, and CREST, Japan Science and Technology Agency, Kawaguchi, Saitama 3320012, Japan

Received: March 17, 2006; In Final Form: April 20, 2006

Undecagold cluster compounds $[Au_{11}(BINAP)_4X_2]^+$ (X = Cl and Br) were synthesized by chemical reduction of the corresponding precursor complexes, $Au_2X_2(BINAP)$, where BINAP represents the bidentate phosphine ligand 2,2′-bis(diphenylphosphino)-1,1′-binaphthyl. The circular dichroism spectra of Au_{11} stabilized by the enantiomers $[Au_{11}(R\text{-BINAP})_4X_2]^+$ and $[Au_{11}(S\text{-BINAP})_4X_2]^+$ exhibited intense and mirror-image Cotton effect, whereas those of Au_{11}^{3+} clusters stabilized by achiral monodentate phosphine ligands did not. The origin of the chiroptical activity of $[Au_{11}(BINAP)_4X_2]^+$ is discussed in the context of the structural deformation of the Au_{11}^{3+} core.

Introduction

Small gold clusters protected or stabilized by organic molecules have gained great interest both in fundamental and application research because they exhibit salient physicochemical properties arising from the small numbers of the core atoms.[1] A number of studies on size-selected gold clusters have demonstrated that their optical,[2] electronic,[3] electrochemical,[4] and catalytic[5] properties are remarkably different from those of bulk gold and evolve perceptively with the core size. Another important structural parameter that affects the basic properties is the interface between the core and the organic molecules.[6−8] For example, it has been demonstrated that magnetic[7] and photoluminescence[8] properties of gold clusters are influenced by the nature of the chemical interaction at the interface. Thus, precise control over the interfacial structure and core size is crucial for imparting new properties to gold clusters and developing them into functional materials.

The induction of chirality on a cluster surface is important, especially for the development of enantioselective nanocatalysts. It is well known that chiral metal surfaces can be obtained by adsorbing chiral molecules, referred to as "chiral modifiers", onto achiral surfaces.[9] Thus, protection by chiral molecules is a reasonable strategy for inducing chirality on metal clusters. Indeed, chiroptical activity has been observed in gold clusters protected by L-glutathione (L-GSH),[2e,f] D-/L-penicillamine (Pen),[10] and (*R*)-/(*S*)-2,2′-bis(diphenylphosphino)-1,1′-binaphthyl (BINAP).[11] Schaaff and Whetten (SW) have suggested, among several possibilities, that the chiroptical activity of Au/L-SG clusters is attributable to helical geometry of the Au core induced by GS ligation.[2f] This chiral core model has been supported by theoretical studies by Garzón and co-workers: strong Au−S interaction distorts the cluster geometry and induces chiroptical activity regardless of the chirality of the thiolates.[12] Recently, another mechanism has been proposed experimentally[10] and theoretically.[13] Yao and co-workers have observed a mirror-image relationship between the circular dichroism (CD) spectra of enantiomers of Au/D-Pen and Au/L-Pen clusters (ϕ = 0.6, 1.2, 1.8 nm).[10] On the basis of kinetic and structural considerations, the optical activity has been ascribed to the dissymmetric field induced by Pen ligation. A theoretical study using a particle-in-a-box model supports the dissymmetric field model: the symmetric metal cores could be optically active when perturbed by a dissymmetric field originating from the adsorbates.[13] In the stabilization by axially chiral BINAP molecules (Chart 1), Tamura and Fujihara have observed chiroptical activity in the gold nanoparticles (1.7±0.4 nm).[11] Despite these extensive studies, the origin of the chiroptical activity of Au clusters remains unclear due mainly to the lack of structural information.

To contribute to the understanding of the origin of cluster chirality, the present study investigates chiroptical activity of undecagold (Au_{11}^{3+}) cluster compounds[14] stabilized by the various phosphines shown in Chart 1: 4,4′,4″-phosphinidynetris(*N*-methylbenzamide) (PTMB) and triphenylphosphine (TPP) are employed as achiral ligands. The phosphine-stabilized Au_{11}^{3+} compound is an ideal system for studying cluster-surface-mediated chiroptical properties because of the extremely high surface-to-volume ratio and well-established morphology of the core. As an example, the structure of well-known $Au_{11}(PTMB)_7X_3$ (**1**) is schematized in Chart 2:[14e] a central gold atom is surrounded by 10 peripheral gold atoms, of which seven and three are, respectively, bonded to phosphines and the pseudohalides X. We first exploit the synthetic method of Au_{11}^{3+} clusters stabilized by (*R*)- and (*S*)-BINAP and then compare their optical activity with those of the conventional $Au_{11}(PTMB)_7X_3$ (ref 14e) and $[Au_{11}(TPP)_8X_2]^+$ (refs 14c,f) clusters. An explanation for high optical activity of Au_{11}^{3+}/BINAP will be proposed on the basis of a chiral core model.[2f,12]

* Corresponding author. Tel: +81-564-55-7351, Fax: +81-564-55-7351. E-mail: tsukuda@ims.ac.jp
[†] Institute for Molecular Science.
[‡] Kinki University.
[§] CREST.

10.1021/jp061670f CCC: $33.50 © 2006 American Chemical Society

CHART 1. Phosphine Ligands Employed in the Present Study

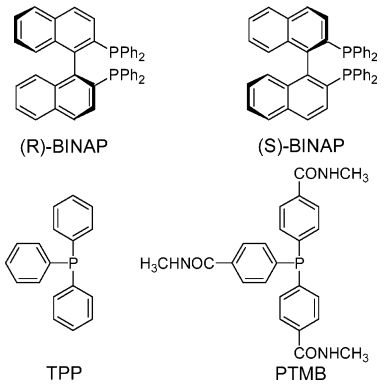

CHART 2. Schematic Representation of $Au_{11}(PTMB)_7Cl_3$ (1)

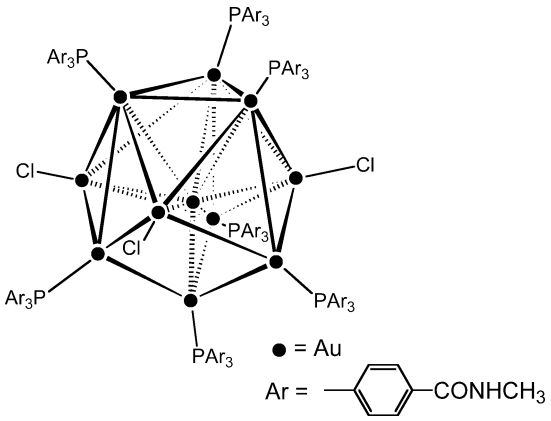

Synthesis

The complexes Au_2Cl_2(*R*-/*S*-BINAP) (**2***R*/**2***S*) were synthesized[15] by following a procedure reported previously.[16] The bromo counterparts Au_2Br_2(*R*-/*S*-BINAP) (**3***R*/**3***S*) were synthesized by using $KAuBr_4$ instead of $NaAuCl_4$.[17] Then, BINAP-stabilized gold clusters (Au/BINAP) were prepared by reducing these Au(I) complexes with $NaBH_4$. Typically, an ethanol solution (400 μL) of $NaBH_4$ (2.60 mg, 0.0686 mmol) was injected into a degassed solution of **2***R*/**2***S* (37.3 mg, 0.0343 mmol) in dichloromethane (37 mL) under vigorous stirring at ambient temperature. After stirring for 2 h, the resulting solution was washed with water and concentrated by rotary evaporation. The residue was reprecipitated from a chloroform solution by hexane to obtain the Au/BINAP clusters. Finally, the precipitate was dried in vacuo to obtain the Au/*R*-/*S*-BINAP clusters (**4***R*/**4***S*) as a dark brown powder. The chemical reduction of **3***R*/**3***S* yields the Au*R*-/*S*-BINAP clusters (**5***R*/**5***S*).

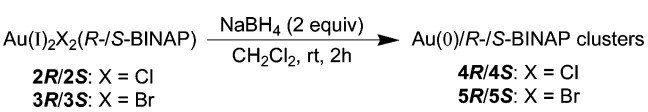

The Au/TPP clusters were prepared by following the synthesis of $[Au_{11}(TPP)_8Cl_2]^+$ reported by Hutchison.[14f] Briefly, an ethanol solution (1 mL) of $NaBH_4$ (7.6 mg, 0.202 mmol) was injected into a degassed mixture of AuCl(TPP) (100 mg, 0.202 mmol) in absolute ethanol (5.5 mL) under vigorous stirring at ambient temperature. After stirring for 2 h, the resulting solution was poured into hexane (100 mL) and allowed to precipitate overnight. The brown solid was collected and washed with hexane (4 × 1.5 mL) and dichloromethane/hexane (1:1, 4 × 1.5 mL). The remaining solid was dissolved in dichloromethane (1 mL) and purified by filtration to obtain Au/TPP clusters (**6**). The preparation by using AuBr(TPP) yielded the Au/TPP clusters (**7**). The $Au_{11}(PTMB)_7Cl_3$ clusters[14b,e] (**1**) were purchased from Nanoprobe Inc.

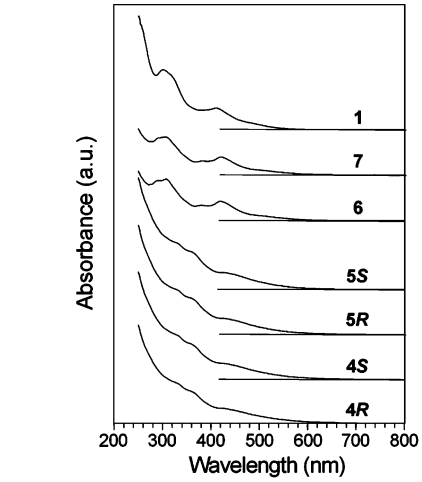

Figure 1. Optical absorption spectra of **1** and **4**−**7**.

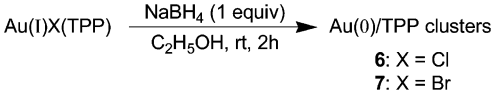

Results and Discussion

Characterization of Au/BINAP and Au/TPP Clusters. Figure 1 shows the optical absorption spectra of the Au/BINAP (**4**/**5**), Au/TPP (**6**/**7**) and $Au_{11}(PTMB)_7Cl_3$ (**1**) clusters. A comparison of **4**/**5** and **6**/**7** reveals that the difference in the halogens does not appreciably affect the electronic structures of the clusters. The **6**/**7** spectra exhibit an onset at ca. 600 nm and peak-like structures in the 300−450 nm range. These spectral features closely resemble those of **1** and $[Au_{11}(TPP)_8Cl_2]^+$ reported by Hutchison.[14f] The similarities strongly suggest that the Au_{11}^{3+} cluster is dominantly formed in **6**/**7**. We tentatively assign **6**/**7** to $[Au_{11}(TPP)_8Cl_2]^+$ (X = Cl and Br). The spectra of **4**/**5** exhibit features similar to those of Au_{11}^{3+} clusters (**1**, **6**, **7**). Figure 2 shows the TEM images of Au/*R*-BINAP (**5***R*) and Au/TPP (**6**). In both samples, highly monodisperse Au clusters with an average diameter of 0.9±0.3 nm are observed. Although evaluating the core sizes precisely from the TEM images is a formidable task, these images are consistent with the formation of the Au_{11}^{3+} cores in **5***R* and **6**. These optical and TEM measurements indicate preferential formation of the Au_{11}^{3+} clusters in **4**−**7**.

More direct information on chemical compositions was obtained by mass spectrometry. Figure 3 shows a typical ESI mass spectrum of **5***R* in the positive-ion mode. The mass spectrum is surprisingly simple. The two major mass peaks are assignable to $[Au_{11}(BINAP)_4Br_2]^+$ and $[Au_{11}(BINAP)_4Br]^{2+}$. The assignments were unequivocally confirmed by the comparison between the experimental and simulated isotopic patterns. The $[Au_{11}(BINAP)_4Br]^{2+}$ ions are thought to be formed from the $[Au_{11}(BINAP)_4Br_2]^+$ parent by losing one Br^- ion during the ESI process. The mass spectrum of **5***S* exhibits the same mass peaks, while those of **4***R*/**4***S* give the corresponding ions of $[Au_{11}(BINAP)_4Cl_2]^+$ and $[Au_{11}(BINAP)_4Cl]^{2+}$.[15,18] These mass spectrometric studies indicate that the $[Au_{11}(BINAP)_4X_2]^+$ clusters (X = Cl and Br) are selectively formed in **4**/**5**. It is worth stressing here that the Au/BINAP (**4**/**5**) and Au/TPP (**6**/

TABLE 1: Summary of Optical and Chiroptical Properties of Au_{11} Clusters

		ϵ ($M^{-1}cm^{-1}$)[a]		$\Delta\epsilon/\epsilon$[b]	
cluster	composition	305 nm	@430 nm	@305 nm	@430 nm
4*R*	$[Au_{11}(BINAP)_4Cl_2]^+$	1.1×10^5	3.7×10^5	-8.7×10^{-4}	1.2×10^{-3}
4*S*		1.1×10^5	3.4×10^5	7.7×10^{-4}	-1.0×10^{-3}
5*R*	$[Au_{11}(BINAP)_4Br_2]^+$	1.1×10^5	3.7×10^4	-9.4×10^{-4}	1.2×10^{-3}
5*S*		1.1×10^5	3.6×10^4	9.0×10^{-4}	-1.1×10^{-3}
6	$[Au_{11}(TPP)_8Cl_2]^+$	9.3×10^4	4.0×10^4		
7	$[Au_{11}(TPP)_8Br_2]^+$	8.5×10^4	4.1×10^4		
1	$Au_{11}(PTMB)_7Cl_3$	1.3×10^5	3.7×10^4		

[a] Molar extinction coefficient. [b] Anisotropy factor.

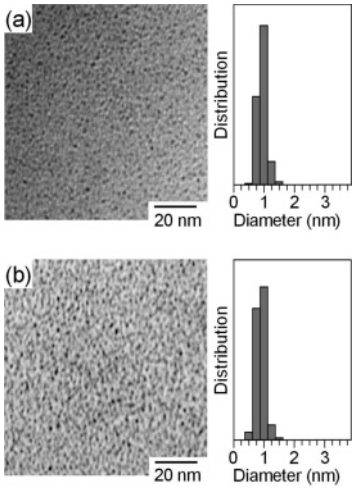

Figure 2. TEM images and core size distributions of (a) **5*R*** and (b) **6**.

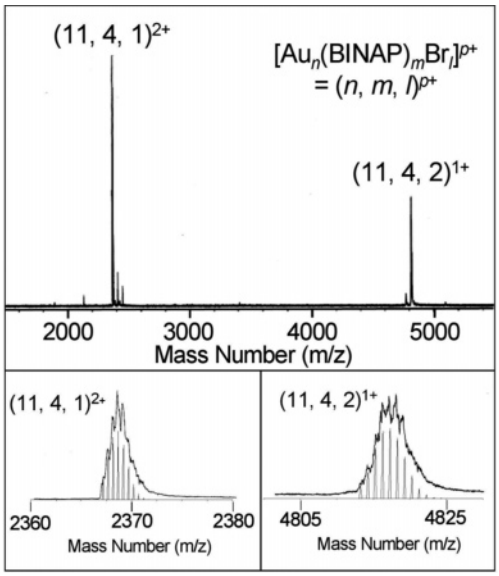

Figure 3. Positive-ion ESI mass spectrum of **5*R***. The bottom panels show the comparisons between the experimental and simulated isotopic patterns of the two main peaks.

7) clusters are composed of the same numbers of gold, phosphine, and halogen. In the framework of the structural model for **1** (Chart 2), it is reasonable to assume that eight peripheral Au atoms are bonded by eight TPP ligands in **6**/**7** or by four BINAP ligands in **4**/**5** and the two remaining Au sites are capped by halogens. The high stability and abundance of these Au_{11}^{3+} cores are well accounted for by the electron counting scheme of Mingos (8 e)[19a] or Pyykkö (18 e).[19b] The molar extinction coefficients of **4**−**7** were calculated by assuming the chemical compositions described above and are

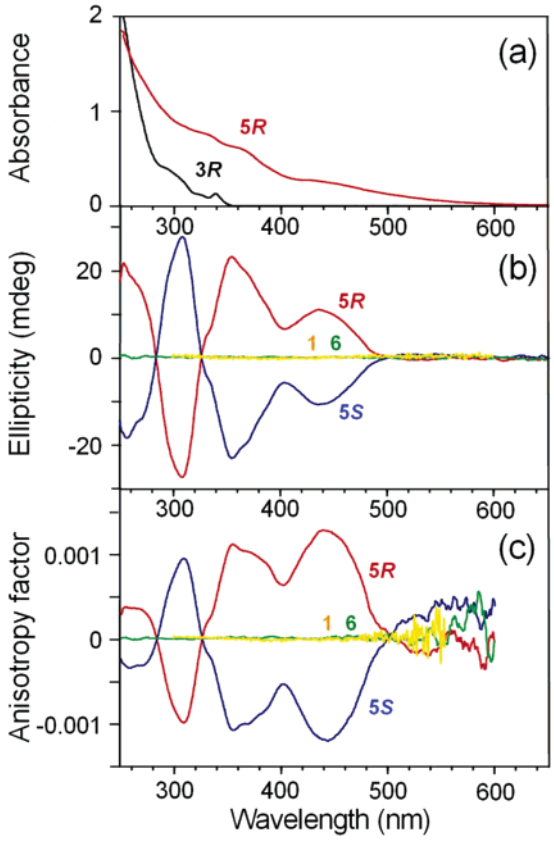

Figure 4. (a) Optical absorption spectra of **3*R***, **5*R*** and (b) ellipticity and (c) anisotropy factor of **1**, **5**, **6**.

tabulated in Table 1. It is found that the molar extinction coefficients are similar, further supporting the formation of the Au_{11}^{3+} clusters in **4**−**7**.

Unfortunately, reliable mass spectral data could not be obtained for the Au/TPP clusters (**6**/**7**) because they are very unstable when dissolved in ethanol or methanol for ESI-MS measurements.[15] The absorption spectra of **6**/**7** in the alcohol dispersion change drastically within 5 min. This suggests a degradation of the clusters, although the reactions involved are not clear at present. The ESI mass spectra of the degraded species were dominated by $Au_{10}(TPP)_8$-based ions, which have also been reported in a previous study by Wang.[20] In contrast, the $[Au_{11}(BINAP)_4X_2]^+$ clusters (**4**/**5**) were found to be more robust than the $[Au_{11}(TPP)_8X_2]^+$ clusters (**6**/**7**) in alcohol solution, presumably due to the bidentate ligation of BINAPs.

Optical Activity of $[Au_{11}(BINAP)_4X_2]^+$ Clusters. We observed that ligand chirality had a dramatic effect on the CD spectra of Au_{11}^{3+} clusters. Figure 4 shows the CD spectra of **1**, **5*R***/**5*S***, and **6**; the ordinates of Figures 4(b) and 4(c) represent the ellipticity and anisotropy factor ($\Delta\epsilon/\epsilon$), respectively. The CD spectra of **5*R***/**5*S*** show intense Cotton effects and a mirror-image relationship in the 250−500 nm range,[21] whereas clusters

1 and **6** stabilized by achiral ligands are not optically active. The anisotropy factors of **5***R*/**5***S* (Table 1) are severalfold larger than those of the Au/SG (refs 2e,f) and Au/Pen (ref 10) clusters with comparable core sizes. The optical activity of **5***R*/**5***S* observed in the 250−500 nm range is associated with the optical transitions localized within the Au_{11}^{3+} core on the basis of the following considerations: (i) the Au(I) precursor **3***R* having no Au−Au bonding is transparent in the wavelength region of 350−500 nm (Figure 4a); (ii) the anisotropy factor of **3***R* in the 250−350 nm range is only at a ppm level,[15] suggesting that the CT transition between the Au_{11}^{3+} core and the ligands and intraligand transitions contribute little to the optical activity of **5**.

Finally, we propose an explanation for the optical activity of $[Au_{11}(BINAP)_4X_2]^+$ based on a chiral core model proposed for thiolate-protected gold clusters.[2f,12] Single-crystal X-ray diffraction studies on various phosphine-stabilized Au_{11} clusters show that the Au_{11}^{3+} core geometries (e.g., distances between adjacent Au atoms) vary significantly with the phosphine ligands used.[14] The flexible nature of the core may stem from the fact that 10 out of the eleven atoms are located on the core surface (Chart 2) and are highly unsaturated. A large strain would be imposed on BINAP ligands anchored on two adjacent sites of Au_{11}^{3+} since the distances of peripheral Au atoms in Au_{11}^{3+} (2.8−3.3 Å)[14] are significantly smaller than that in the precursor (∼6.0 Å). This strain would cause the core to deform so that CD activity is associated with the optical transitions within the core. However, we cannot rule out a possibility that a dissymmetric field may play a role. We must await further experimental and theoretical studies on $[Au_{11}(BINAP)_4X_2]^+$ structures to elucidate the origin of the chirality.

Summary

We report herein a facile synthesis of chemically pure $[Au_{11}(BINAP)_4X_2]^+$ (X = Cl and Br) on a preparative scale by chemical reduction of the corresponding precursor complexes, $Au_2X_2(BINAP)$. The enantiomers $[Au_{11}(R\text{-}BINAP)_4X_2]^+$ and $[Au_{11}(S\text{-}BINAP)_4X_2]^+$ gave excellent mirror-image CD spectra, whereas $[Au_{11}(TPP)_8X_2]^+$ and $Au_{11}(PTMB)_7Cl_3$ did not. The flexible nature of the Au_{11}^{3+} core suggests that the CD activity of $[Au_{11}(BINAP)_4X_2]^+$ originates from the core deformation due to BINAP ligation.

Acknowledgment. The authors wish to thank Prof. Y. Uozumi (IMS) for providing access to the mass spectrometer, polarimeter, and melting-point apparatus used in this study. Y.Y. acknowledges the Inoue Foundation for Science, Japan for providing a research fellowship. The present work was supported by Grants-in-Aid for Scientific Research (No. 769 and 90262104) and by the CREST program sponsored by JST.

Supporting Information Available: Details of the synthesis and CD spectra of **3**, ESI mass and CD spectra of **4**, absorption spectra of **5** and **6** in methanol. This material is available free of charge via the Internet at http://pubs.acs.org.

References and Notes

(1) Daniel, M.-C.; Astruc, D. *Chem. Rev.* **2004**, *104*, 293 and references therein.

(2) (a) Alvarez, M. M.; Khoury, J. T.; Schaaff, T. G.; Shafigullin, M. N.; Vezmar, I.; Whetten, R. L. *J. Phys. Chem. B* **1997**, *101*, 3706. (b) Schaaff, T. G.; Shafigullin, M. N.; Khoury, J. T.; Vezmar, I.; Whetten, R. L.; Cullen, W. G.; First, P. N.; Gutiérrez-Wing, C.; Ascensio, J.; Jose-Yacamán, M. J. *J. Phys. Chem. B* **1997**, *101*, 7885. (c) Hostetler, M. J.; Wingate, J. E.; Zhong, C.-J.; Harris, J. E.; Vachet, R. W.; Clark, M. R.; Londono, J. D.; Green, S. J.; Stokes, J. J.; Wignall, G. D.; Glish, G. L.; Porter, M. D.; Evans, N. D.; Murray, R. W. *Langmuir* **1998**, *14*, 17. (d) Gutiêrrez, E.; Powell, R. D.; Furuya, F. R.; Hainfeld, J. F.; Schaaff, T. G.; Shafigullin, M. N.; Stephens, P. W.; Whetten, R. L. *Eur. Phys. J. D* **1999**, *9*, 647. (e) Schaaff, T. G.; Whetten, R. L. *J. Phys. Chem. B* **1999**, *103*, 9394. (f) Schaaff, T. G.; Whetten, R. L. *J. Phys. Chem. B* **2000**, *104*, 2630. (g) Negishi, Y.; Takasugi, Y.; Sato, S.; Yao, H.; Kimura, K.; Tsukuda T. *J. Am. Chem. Soc.* **2004**, *126*, 6518. (h) Negishi, Y.; Nobusada, K.; Tsukuda, T. *J. Am. Chem. Soc.* **2005**, *127*, 5261.

(3) Zhang, P.; Sham, T. K. *Phys. Rev. Lett.* **2003**, *90*, 245502.

(4) Chen, S.; Ingram, R. S.; Hostetler, M. J.; Pietron, J. J.; Murray, R. W.; Schaaff, T. G.; Khoury, J. T.; Alvarez, M. M.; Whetten, R. L. *Science* **1998**, *280*, 2098.

(5) (a) Tsunoyama, H.; Sakurai, H.; Ichikuni, N.; Negishi, Y.; Tsukuda, T. *Langmuir* **2004**, *20*, 11293. (b) Tsunoyama, H.; Sakurai, H.; Negishi, Y.; Tsukuda, T. *J. Am. Chem. Soc.* **2005**, *127*, 9374. (c) Burato, C.; Centomo, P.; Pace, G.; Favaro, M.; Prati, L.; Corain, B. *J. Mol. Catal. A: Chem.* **2005**, *238*, 26. (d) Haruta, M. *Nature* **2005**, *437*, 1098.

(6) Zhang, P.; Sham, T. K. *Appl. Phys. Lett.* **2002**, *81*, 736.

(7) (a) Crespo, P.; Litrán, R.; Rojas, T. C.; Multigner, M.; de la Fuente, J. M.; Sánchez-López, J. C.; García, M. A.; Hernando, A.; Penadés, S.; Fernández, A. *Phys. Rev. Lett.* **2004**, *93*, 087204. (b) Yamamoto, Y.; Miura, T.; Suzuki, M.; Kawamura, N.; Miyagawa, H.; Nakamura, T.; Kobayashi, K.; Teranishi, T.; Hori, H. *Phys. Rev. Lett.* **2004**, *93*, 116801.

(8) (a) Lee, D.; Donkers, R. L.; Wang, G.; Harper, A. S.; Murray, R. W. *J. Am. Chem. Soc.* **2004**, *126*, 6193. (b) Zheng, J.; Zhang, C.; Dickson, R. M. *Phys. Rev. Lett.* **2004**, *93*, 077402.

(9) (a) Blaser, H.-U.; Jalett, H.-P.; Müller, M.; Studer, M. *Catal. Today* **1997**, *37*, 441. (b) Lorenzo, M. O.; Baddeley, C. J.; Muryn, C.; Raval, R. *Nature* **2000**, *404*, 376. (c) Schunack, M.; Lægsgaard, E.; Stensgaard, I.; Johannsen, I.; Besenbacher, F. *Angew. Chem., Int. Ed.* **2001**, *40*, 2623. (d) Switzer, J. A.; Kothari, H. M.; Poizot, P.; Nakanishi, S.; Bohannan, E. W. *Nature* **2003**, *425*, 490.

(10) Yao, H.; Miki, K.; Nishida, N.; Sasaki, A.; Kimura, K. *J. Am. Chem. Soc.* **2005**, *127*, 15536.

(11) Tamura, M.; Fujihara, H. *J. Am. Chem. Soc.* **2003**, *125*, 15742.

(12) (a) Garzón, I. L.; Reyes-Nava, J. A.; Rodríguez-Hernández, J. I.; Sigal, I.; Beltrán, M. R.; Michaelian, K. *Phys. Rev. B* **2002**, *66*, 073403. (b) Garzón, I. L.; Beltrán, M. R.; González, G.; Gutíerrez-González, I.; Michaelian, K.; Reyes-Nava, J. A.; Rodríguez-Hernández, J. I. *Euro. Phys. J. D* **2003**, *24*, 105. (c) Román-Velázquez, C. E.; Noguez, C.; Garzón, I. L. *J. Phys. Chem. B* **2003**, *107*, 12035.

(13) Goldsmith, M.-R.; George, C. B.; Zuber, G.; Naaman, R.; Waldeck, D. H.; Wipf, P.; Beratan, D. N. *Phys. Chem. Chem. Phys.* **2006**, *8*, 63.

(14) (a) Albano, V. G.; Bellon, P. L.; Manassero, M.; Mansoni, M. *J. Chem. Soc., Chem. Commun.* **1970**, 1210. (b) Bartlett, P. A.; Bauer, B.; Singer, S. J. *J. Am. Chem. Soc.* **1978**, *100*, 5085. (c) Vollenbroek, F. A.; Bour, J. J.; Van der Velden, J. W. A. *Rec. Trav. Chim. Pays-Bas* **1980**, *99*, 137. (d) Smith, J. M. M.; Bour, J. J.; Vollenbroek, F. A.; Beurskens, P. T. *J. Cryst. Spec. Rec.* **1983**, *13*, 1986. (e) Safer, D.; Lizann, B.; Leigh, J. S. *J. Inorg. Biochem.* **1986**, *26*, 77. (f) Woehrle, G. H.; Warner, M. G.; Hutchison, J. E. *J. Phys. Chem. B* **2002**, *106*, 9979. (g) Yang, Y.; Chen, S. *Nano Lett.* **2003**, *3*, 75. (h) Nunokawa, K.; Onaka, S.; Yamaguchi, T.; Ito, T.; Watase, S.; Nakamoto, M. *Bull. Chem. Soc. Jpn.* **2003**, *76*, 1601.

(15) See Supporting Information.

(16) Muñoz, M. P.; Adrio, J.; Carretero, J. C.; Echavarren, A. M. *Organometallics* **2005**, *24*, 1293.

(17) Selected data for compound **2*R***; White crystalline powder: mp > 280 °C (decomp); ^{1}H NMR (500 MHz, $CDCl_3$) δ 8.20 (d, J = 8.6 Hz, 2H), 7, 98 (d, J = 7.9 Hz, 2H), 7.62−7.57 (m, 4H), 7.50 (t, J = 9.2 Hz, 4H), 7.43−7.35 (m, 4H), 7.35−7.23 (m, 8H), 7.22−7.13 (m, 4H), 6.99 (t, J = 7.63 Hz, 2H), 6.76 (d, J = 8.6 Hz, 2H); ^{13}C NMR (125 MHz, $CDCl_3$) δ 143.36 (dd, $J(^{13}C\text{-}^{31}P)$ = 16.0 Hz, $J(^{13}C\text{-}^{31}P)$ = 7.9 Hz) 134.85 (d, $J(^{13}C\text{-}^{31}P)$ = 14.4 Hz), 134.62 (d, $J(^{13}C\text{-}^{31}P)$ = 19.5 Hz), 133.99 (d, $J(^{13}C\text{-}^{31}P)$ = 12.4 Hz), 133.71 (d, $J(^{13}C\text{-}^{31}P)$ = 13.4 Hz) 131.75−130.90, 130.75 130.45−129.60, 129.35−128.44, 128.41, 127.68, 127.26, 126.60, 126.33 (d, $J(^{13}C\text{-}^{31}P)$ = 2.0); ^{31}P NMR (202.5 MHz, $CDCl_3$) δ 25.77 (s). MALDI-TOF-MS for $C_{44}H_{32}Au_2Br_2P_2$: m/z calcd, 1096.5 $[M\text{-}Br]^+$; Found: 1097.0; $[\alpha]^{22}_D$ = −27 (c = 0.050, $CHCl_3$): for compound **2*S***; mp, ^{1}H, ^{13}C, and ^{31}P NMR and MALDI-TOF-MS are essentially the same with **2*R***; $[\alpha]^{22}_D$ = +27 (c = 0.050, $CHCl_3$).

(18) The ESI mass spectra of **4** are contaminated by Br impurities whose source could not be identified at present.

(19) (a) Mingos, D. M. P. *Chem. Soc. Rev.* **1986**, *15*, 31. (b) Pyykkö, P. *Angew. Chem., Int. Ed.* **2004**, *43*, 4412.

(20) Zhang, H.-F.; Stender, M.; Zhang, R.; Wang, C.; Li, J.; Wang, L.-S. *J. Phys. Chem. B* **2004**, *108*, 12259.

(21) The CD spectra in Figure 4 are similar to those of the Au/BINAP nanoparticles with diameters of 1.7±0.4 nm reported in ref 11. We interpret that the CD spectra in ref 11 originate from the optically active Au_{11}/BINAP clusters contained as minor species in their samples or overestimation of the core sizes due to enhanced imaging of larger clusters.